ACS Photonics

Letter

pubs.acs.org/journal/apchd5

Functionalized Hydrogel on Plasmonic Nanoantennas for Noninvasive Glucose Sensing

Martin Mesch,[†] Chunjie Zhang,[‡] Paul V. Braun,[‡] and Harald Giessen*[,†]

[†]4th Physics Institute and Research Center SCoPE, University of Stuttgart, Pfaffenwaldring 57, 70569 Stuttgart, Germany

[‡]Department of Materials Science and Engineering, Beckman Institute for Advanced Science and Technology, and Frederick Seitz Materials Research Laboratory, University of Illinois at Urbana−Champaign, 1304 West Green Street, Urbana, Illinois 61801, United States

ABSTRACT: Plasmonic nanostructures are intensely investigated as sensors due to their high sensitivity to changes in their nearest dielectric environment. However, additional steps have to be taken to provide specificity for a particular analyte. Here, gold nanoantennas are coated with a thin layer of a boronic acid functionalized hydrogel, which reversibly swells in the presence of glucose. This process is especially sensitive to low glucose concentrations and allows for measurement of values in the physiological millimolar range. The boronic acid is highly specific to glucose, and large molecules, such as proteins, which could cause possible disturbances to the measurements, are successfully blocked from the plasmonic sensing volume by the hydrogel film. Our concept is thus suited to detect physiological glucose levels in the tear liquid under the presence of ambient proteins using functionalized plasmonic sensors on contact lenses at eyesafe wavelengths for optical readout.

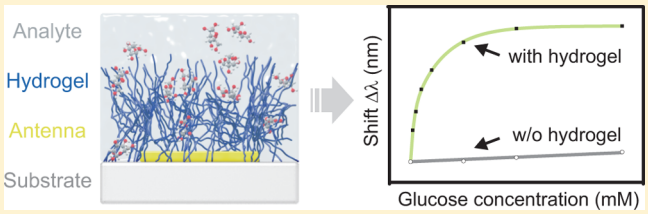

KEYWORDS: *plasmon, glucose, sensing, hydrogel, functionalization, nanoantennas*

In the past few years, a variety of plasmonic metal nanostructures has been investigated with respect to application as sensors based on localized surface plasmon resonances (LSPR). Many groups studied holes in metal films, nanoantennas, and arrangements of particles, exhibiting Fano-resonances or chiral properties to exploit the large sensitivity, small sensing volumes, and high integration density provided by such systems.[1−11] Others focused on fabrication methods to generate high quality, large area arrays, for example, nanosphere lithography, nanoimprint lithography, or nanostencil lithography.[12−14] Additional parameters, such as efficient delivery of analytes to the sensor, have also been subject to optimization.[15] As known from experiments, the exact optical properties, such as the resonance positions, depend strongly on the dielectric vicinity of the metal structures. Since the dielectric function is, however, influenced by almost any change in the surrounding material, an additional component is needed to provide selectivity.

Independent of the structure in use, it is always a challenge to limit the otherwise very general response, which includes all changes in the effective refractive index of the environment, to a preferably single desired analyte. One established method is to directly attach selected molecules to the metal, e. g. to gold via a thiol group, which will in turn bind the desired analyte molecules and cause the change in the environment of the antennas. In experiments, the analyte solution is guided to the sensitive area and allowed to react for a specific duration, before flushing the sample with a clean solution to wash away everything that is not bound to the gold structures. Subsequently, the resonance shift caused by the few additional molecules can be detected. The fact that this is a very diminutive refractive index change can to some extent be overcome as it is confined to the region with the highest field enhancement. Depending on the molecules, the analyte binding process may be permanent and, hence, the sensor can be used only once. In the realm of biological sensing, immobilized antibodies are a widely used technique to bind the respective antigens to the sensor surface for detection.[16] For more general chemical sensing, direct functionalization, self-assembled monolayers with functional end groups, or embedding plasmonic structures in thin layers of chemically reactive materials are applicable methods.[17−22] Moreover, the vibrational signals of molecules in the infrared fingerprint region can be used by surface-enhanced infrared absorption (SEIRA) spectroscopy to identify a broad range of substances, while still taking advantage of the enhanced electromagnetic fields of plasmonic nanoantennas.[23] Similarly, Raman spectroscopy can benefit from plasmonically enhanced surfaces and also allow for specific detection of analytes.[24]

Among the many possible sensor designs, one class of nonplasmonic sensor concepts that has been significantly developed is based on hydrogels, which are hydrophilic cross-linked polymer networks soaked with water. Hydrogels are used in applications ranging from contact lenses to drug delivery and biosensing. Hydrogels can be functionalized to respond to changes in temperature, pH, ionic strength, metal ions, antigens, and the presence of a number of biomole-

Received: January 7, 2015
Published: March 19, 2015

DOI: 10.1021/acsphotonics.5b00004
ACS Photonics 2015, 2, 475−480

cules.[25−32] The response, typically a reversible volume change of the gel, can then be read out as the sensor signal.

In our approach, we combine the high sensitivity of plasmonic nanoantennas with the advantages provided by a functionalization layer of a hydrogel. This combination provides specificity for glucose, even in the presence of large proteins, and response to glucose is reversible. However, it is important to note that our sensor concept is not limited to glucose, but can be adapted without any restrictions to many different analytes by choosing the appropriate hydrogel.

RESULTS AND DISCUSSION

We fabricated gold nanoantennas on a glass substrate which provide resonances in the near-infrared spectral region (Figure 1b) and covered them with a thin layer of a hydrogel similar to the recipe used by Lee et al.[33] Preparation details are given in the Experimental Section. The simple nanostructure was chosen due to its easy tunability with respect to resonance wavelength and resonance strength and its reliable, reproducible, and fast fabrication. The dimensions arise from a design intended to exhibit a resonance in an "eye-safe" wavelength regime, but not further to the infrared to avoid stronger absorption by the water film. For future experiments, EIT-type or Fano resonances with narrow spectral line width and even higher sensitivity, yet more complex shapes, could also be considered.[34]

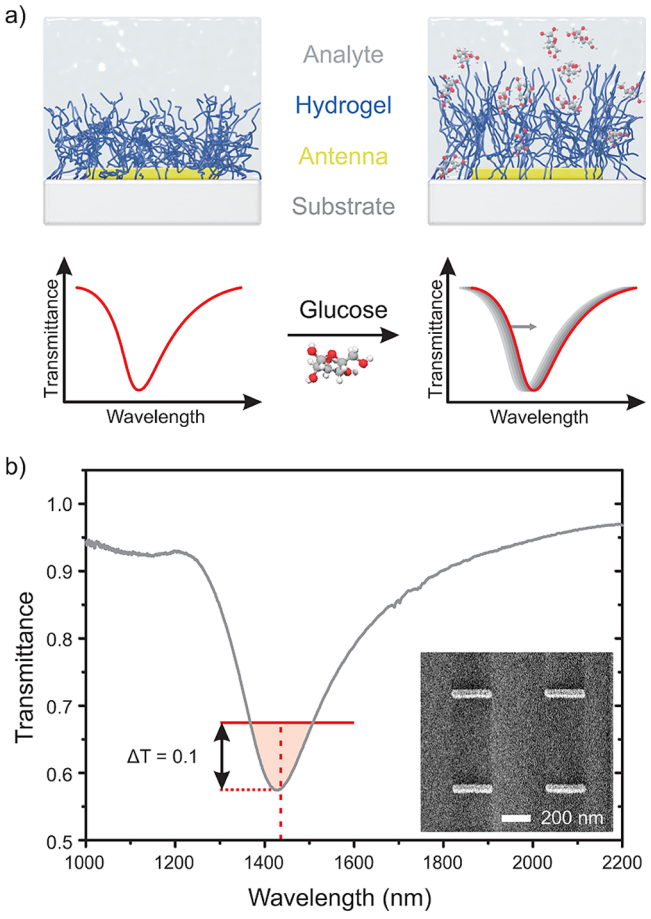

Figure 1. (a) Schematic layout and sensor principle. The plasmonic structures are covered with a 1 μm layer of a hydrogel. Tailored functionalization with a phenylboronic acid causes the hydrogel to swell in the presence of glucose molecules. The resulting change in its effective refractive index leads to a detectable shift at the antenna's resonance. (b) Exemplary spectrum of the hydrogel covered antennas with illustration of the threshold and corresponding centroid wavelength used for tracking the resonance shift. The inset depicts a representative SEM picture of the fabricated gold nanostructures before hydrogel application.

The hydrogel is a cross-linked hydrophilic polymer which is swollen with water. Several sites in the polymer chains are replaced with a phenylboronic acid. This acid forms a negatively charged complex with 1,2-*cis*-diols, such as glucose, which subsequently leads to an influx of water into the hydrogel. As the hydrogel swells, the ratio of polymer to water in the gel changes, and thus the gel's effective refractive index changes. This refractive index change can be observed as a shift in the plasmon resonance (Figure 1a). To effectively use the enhanced near-fields around the gold antennas, but at the same time keep the hydrogel thin enough to allow for fast diffusion processes and thus for reasonable response times, the polymer layer was fabricated with a thickness of 1 μm following the procedures provided in the Experimental Section.

To investigate not just the total resonance shift, but also its temporal behavior, a spectrum was taken every 30 s during a measurement series with glucose concentrations from 0 to 100 mM. The resonance position, evaluated by a centroid detection method (cf. Experimental Section), exhibits distinct shifts for every concentration step up to 50 mM, when plotted over time (Figure 2).

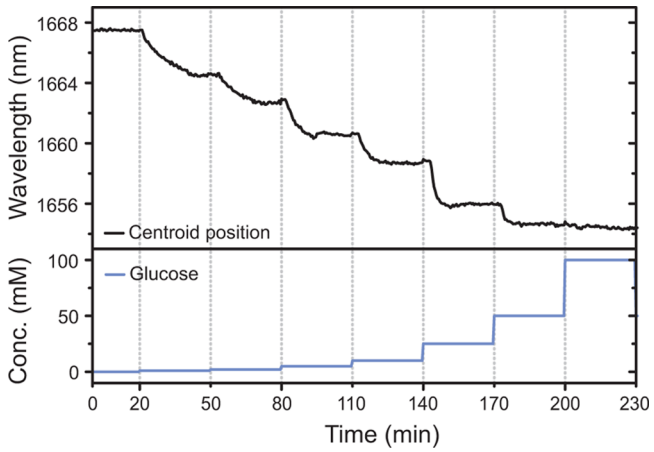

Figure 2. Temporal evolution of the resonance position (determined by its centroid wavelength) for varying glucose concentrations in the analyte solution from 0 to 100 mM.

Extracting the equilibrium positions of the centroid wavelength for all concentrations from the time trace in Figure 2 yields the expected saturation behavior (Figure 3a), as the majority of the boronic acid functionalities in the hydrogel become bound to glucose. When compared to the same glucose concentrations measured on a plasmonic substrate without the hydrogel film, the hydrogel clearly exhibits a much better response to low concentrations. On the bare gold antennas, the refractive index is changed by just the additional glucose molecules in the solution, which leads to only a small signal. In the case of the hydrogel covered antennas, the increasing water content and the relatively high difference in the refractive indices of water and the polymer induce a much more pronounced change. The large shifts for low glucose concentrations, including the physiological range, support the

DOI: 10.1021/acsphotonics.5b00004
ACS Photonics 2015, 2, 475−480

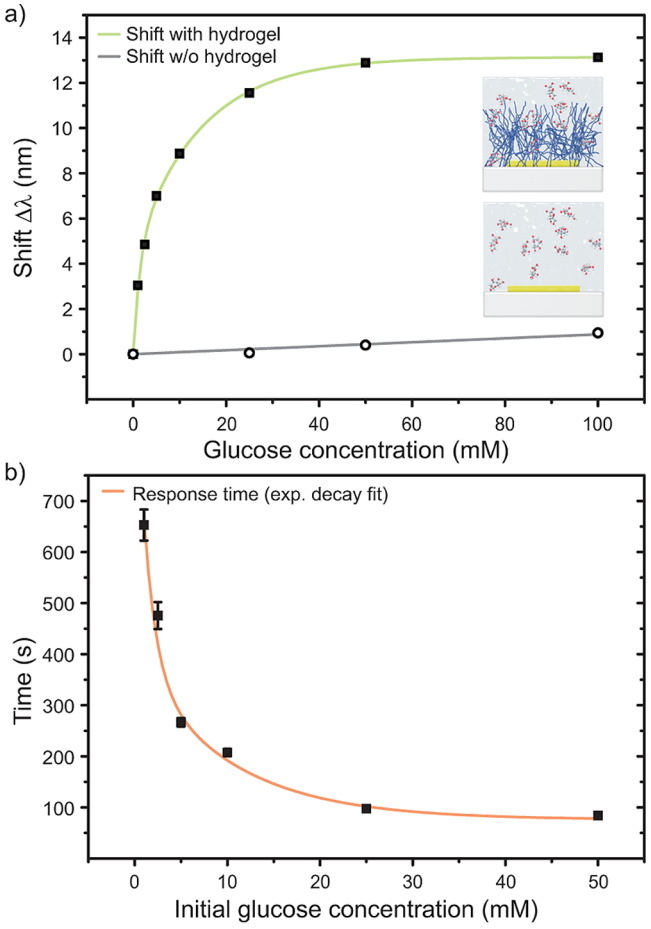

Figure 3. (a) Centroid wavelength shift $\Delta\lambda$ displays the expected saturation as all functionalized sites in the hydrogel become occupied by glucose molecules. In the low concentration regime, the hydrogel exhibits a distinct signal compared to the shift on bare gold structures. (b) Response times, as obtained from exponential fits to Figure 2, are high for low concentrations and decrease when more water in the polymer allows for faster diffusion processes at high concentrations.

possible application of the sensor for human blood glucose levels. For optimization purposes or other applications, the sensing range can be adapted by smart engineering of the polymer.[35]

Figure 2 indicates that the sensor response time differs for varying concentrations. Therefore, exponential decay curves were fitted to the particular sections of the time trace corresponding to every single glucose concentration. The sudden offset of 0.24 nm after 95 min, attributed to an external disturbance, was compensated for the fit. Figure 3b shows the resulting half-life values, which exhibit a trend inverse to the shift. This can be explained by considering the hydrogel water content in the equilibrium state for varying glucose concentrations. For low values, the polymer contains just a small amount of water, limiting the rate of diffusion of glucose molecules into the film. If there already is some glucose, and hence water, present in the polymer, the transport of new glucose molecules can take place much faster. To overcome this issue, a preswollen hydrogel could be used to particularly favor the important range of small concentration values, yet, at the expense of the detectable maximum range.

As one is generally able to detect shifts when they exceed the noise of the measurement, the current detection limit can be estimated. Calculating the mean absolute deviation of the measurement data from the exponential fits to Figure 2 gives a noise level for the spectral shift as low as 0.1 nm. Linear extrapolation of the values for 2.5 and 1 mM glucose relates to a concentration of 0.05 mM at 0.1 nm shift. Hence, the approximated limit of detection is a concentration of 50 μM.

Another advantage of this chemistry is the reversibility of all the sensing processes. Since the reaction between glucose and the phenylboronic acid quickly reaches a dynamic equilibrium and water can get in and out of the hydrogel freely, changes in the glucose concentration in the overlying fluid quickly result in changes in the water content of the hydrogel. The polymer itself is tightly bound to the substrate, and the gold antennas are not part of any chemical processes, so the sensors are stable. Hence, the plasmonic resonance wavelength reversibly shifts back to the original value (Figure 4). In the measurement, two

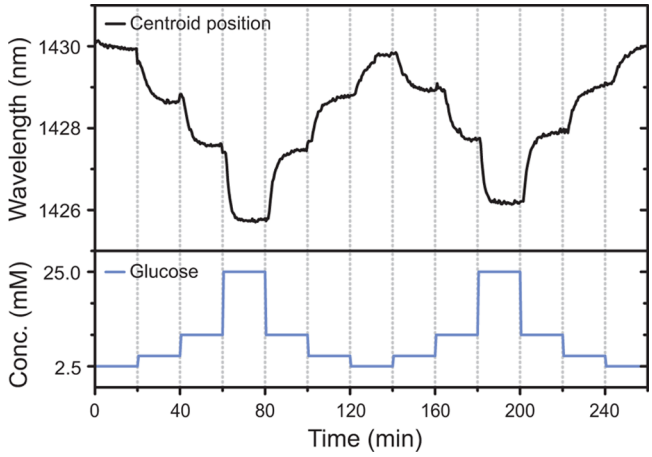

Figure 4. All involved processes are reversible and allow for continuous measurements, without any flushing or regeneration between different concentrations. After two cycles with varying glucose contentrations between 2.5 and 25 mM, the centroid position shifts back to its initial value.

full cycles with glucose concentrations ranging between 2.5 and 25 mM could be achieved, without any flushing or regeneration steps needed in-between. The still visible slight redshift in the second cycle has to be included in investigations regarding long-term stability of the sensor. As a redshift of the resonance corresponds to an increasing refractive index, disintegration or delamination of the polymer layer can already be excluded at this point.

In more application-related environments, proteins are one of the main issues a sensor of this type will need to deal with. To simulate such a less clean sensing environment, we intentionally contaminated our analyte solutions with 0.5 mM albumin. This protein has a molecular weight of approximately 66 kDa, and is also present in the human organism at similar concentrations. For safety reasons, bovine serum albumin (BSA) was used in the experiments. To demonstrate the specificity of the hydrogel layer, measurements were carried out on two otherwise identical samples, with just one of them coated with the hydrogel film. Due to the small glucose signal on the bare gold antennas (see Figure 3), the glucose concentrations in the analyte solutions were increased by a factor of 4 for the experiment on the respective sample, so that clear visibility of the single steps is maintained.

DOI: 10.1021/acsphotonics.5b00004
ACS Photonics 2015, 2, 475−480

Without the hydrogel layer, the bulky protein molecules, as expected, produce a large shift in the signal (Figure 5a).

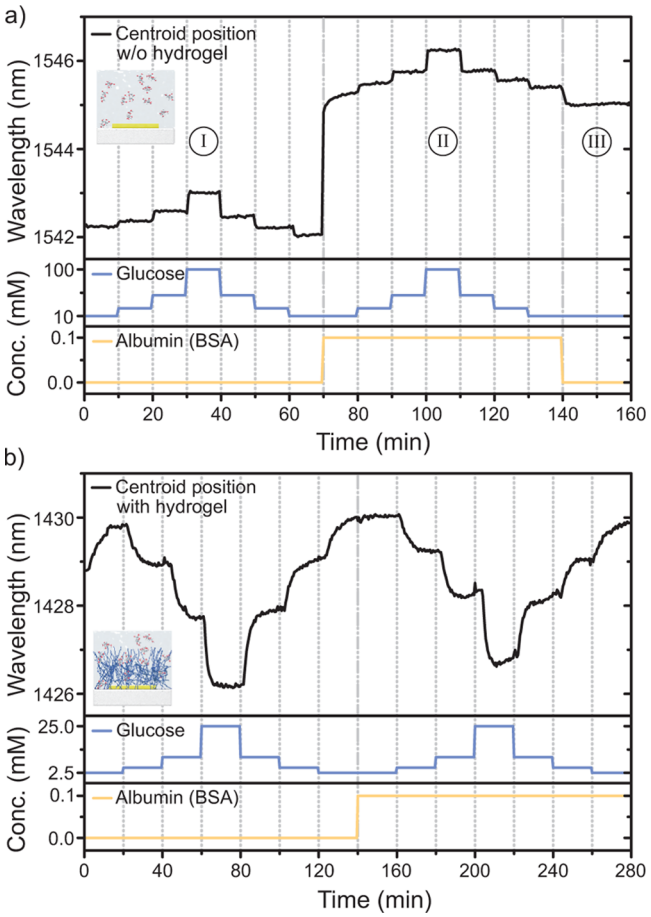

Figure 5. (a) Without the hydrogel film, the large and sticky (BSA) proteins cause a large shift (transition regions I to II), which does not recover when returning to clean glucose solutions (region III). (b) By adding a 1 μm layer of hydrogel on top of the gold nanoantennas, the proteins can be kept out of the sensitive region around the plasmonic structures and glucose concentrations can be detected without major disturbances.

Although the concentration of BSA is much lower than that of glucose (0.5 mM compared to 10−100 mM), the signal induced by the protein exceeds the shift caused by glucose because of the ratio of about 370:1 of their molecular weights. Furthermore, the sticky protein covers the plasmonic structures and prevents the resonance from returning to is initial position when changing back to pristine solutions without BSA. The hydrogel, in contrast, prevents the macromolecules from entering the sensitive area around the gold antennas and is still able to expand and contract as the glucose concentration changes to allow for clear readings of the injected glucose concentrations.

CONCLUSIONS

A layer of functionalized hydrogel is used to coat an array of gold nanoantennas to provide a plasmonic sensor for glucose molecules. The hydrogel polymer contains a phenylboronic acid, which reacts with the glucose molecules and leads to an effective refractive index change of the hydrogel due to the resultant increase in the water content of the hydrogel. When detecting the changes via investigation of the plasmon resonance shift, a clear signal is revealed in comparison to the changes induced by the glucose molecules alone. This allows for concentrations in the physiological range to be measured. Furthermore, the temporal behavior of the system was analyzed as well as the reversibility of the process. The influence of proteins on the measurement was studied, with the results suggesting the polymer is able to suppress negative effects.

Similar types of experiments have been carried out using other techniques, for example, surface plasmon resonance spectroscopy (SPR) or quartz crystal microbalances (QCM).[36−38] While the examined sensing ranges are mostly comparable, our concept provides the additional benefit of a simple contactless optical setup, a sensing area down to the single particle level, and the inherent filtering properties of the hydrogel. QCM measurements, however, are not noninvasive, and SPR measurements depend crucially on the incidence angle of light. Localized plasmons, as in our setup, display the required angle insensitivity required for tear liquid measurements on an eye.

The biocompatibility of the hydrogel and gold nanostructures also encourages a future application in medical devices, such as purely passive contact lenses (which are often hydrogel-based) for noninvasive glucose sensing in the tear liquid. For this purpose, a phenylboronic acid even more specifically reacting with glucose at physiological pH values, such as presented by Alexeev et al., could be used.[39]

In summary, the combination of plasmonic structures with functionalized hydrogels appears to provide an interesting paradigm for biosensing and extends the pool of options to adapt plasmonic sensors to the needs of different applications.

EXPERIMENTAL SECTION

Materials. Hydroxyethyl methacrylate (HEMA), ethylene glycol dimethacrylate (EGDM), Irgacure 651 photoinitiator (IR-651), methacryloxypropyltrimethoxysilane (MPMS), (tridecafluoro-1,1,2,2-tetrahydrooctyl) dimethylchlorosilane (FDCS), 2-(cyclohexylamino)ethanesulfonic acid (CHES), 3-aminophenylboronic acid (APBA), and bovine serum albumin (BSA) were used as received. *N*-3-Acrylamidophenylboronic acid (AAPBA) was synthesized according to the procedure of Li et al.[40] A 2.6% (w/v) aqueous suspension of Polysciences Polybead Microspheres with a diameter of 1.025 μm was diluted with ethanol to be used for spin-coating. Poly(dimethylsiloxane) (PDMS) elastomer kit was ordered from VWR International.

Nanostructure Fabrication. Samples were prepared on 10 × 10 × 0.5 mm^3 glass slides. After cleaning with acetone and isopropanol in an ultrasonic bath, a standard electron beam lithography process with positive resist (PMMA) was used for the nanostructure fabrication. Three 100 × 100 μm^2 arrays of nanoantennas, with a length of 310 nm, a width of 60 nm, and a periodicity of 700 nm in each direction, were written at the center of the substrate. Following the exposure, the resist was developed and a 2 nm Cr adhesion layer was evaporated before a 40 nm film of gold. A subsequent lift-off procedure removed the unexposed resist and thus the gold in the areas around the structures. To get rid of any residual PMMA the samples were treated with oxygen plasma (Technics 100-E Plasma System) at an oxygen pressure of 1 Torr and a power of 250 W for 3 min, and finally rinsed with acetone and isopropanol.

DOI: 10.1021/acsphotonics.5b00004
ACS Photonics 2015, 2, 475−480

To verify the manufacturing process, one of a batch of samples was imaged with a Hitachi S-4800 scanning electron microscope (SEM).

Hydrogel. Substrates with already fabricated gold antennas on top were submerged in 2 mM MPMS in toluene overnight, to introduce acrylate groups to the surface. Another set of glass slides was treated in a 2 mM solution of FDCS in chloroform during the same time to render them hydrophobic for their subsequent application as covers in the polymerization process. All slides were rinsed with isopropanol afterward. Prior to this treatment, the surface of the covers was roughened using fine grinding powder, to avoid thin film interferences in the spectroscopic investigations of the final hydrogel layer.

A mixture of HEMA (458 mg), EGDM (7.5 mg), AAPBA (45.35 mg), and IR-651 (19.7 mg) was prepared and slightly shaken until all ingredients were fully dissolved.

Polystyrene beads were spin-coated onto the samples at 2000 rpm to serve as a spacer. Afterward, a small drop of the monomer solution was pipetted to the center of the substrate and covered with one of the top slides. Gentle movement of the cover under light pressure using the finger tip made the excess liquid to leak from the sides. Two clamps sustained the pressure and kept everything in place while the polymerization was initiated and allowed to continue for 15 min under UV light. The cover was then demounted, and the cured polymer was removed everywhere, except from a 1.5×0.5 mm^2 area above the gold nanoantennas. This had to be done manually with the help of a razor blade and microscope. Finally, the glass regions of the sample were again cleaned with isopropanol.

Measurements. For the measurements we used a custom-made three layer microfluidic cell. The sample holder was designed as an adapter for the spectrometer, with an indent for the substrates to be flush with its surface. A 3 mm layer of PDMS defined the microfluidic system and sealed it in combination with the sample's glass surface. This rubber-like slice featured a 70 μm thick channel with inlet and outlet tubing on its ends directly cast into the silicone. The respective mold was fabricated through optical lithography in MicroChem SU-8 2025 resist on a silicon wafer.

Buffer solution for all measurements was prepared by mixing CHES (1.555 g) and NaCl (0.707 g) in 75 mL of DI water. Monitoring the changes with a pH-meter, 1 M NaOH was added until it reached pH 9.0 and the solution was filled up to 100 mL. In case of the studies with proteins, 3.3 g of BSA was added to the buffer solution.

For analyte solutions, 180.16 mg of D(+)-glucose was dissolved in 5 mL of buffer solution, subsequently extending it to 10 mL to form a 100 mM glucose solution. All other concentrations, namely, 50, 25, 10, 5, 2.5, and 1 mM, were obtained by serial dilution.

Fresh and dry samples were installed into the microfluidic cell and flushed overnight with the first analyte solution to be measured. A constant flow of about 30 μL/min was ensured by placing a reservoir ~20 cm above and the outlet in a beaker ~20 cm below the cell.

Transmittance spectra were recorded using a Fourier transform infrared spectrometer (Bruker Vertex 80), extended by an infrared microscope (Bruker Hyperion 2000). Appropriate for the spectral region, we choose a CaF_2 beam splitter and a liquid-nitrogen-cooled mercury cadmium telluride (MCT) detector in the setup. Additionally, an infrared polarizer set the polarization of the incident light, and an aperture confined the beam to a $\sim 120 \times 120$ μm^2 area. Reference measurements for normalization were taken prior to every single sample measurement at a point next to the gold nanoantennas, that is, through cell, hydrogel film, and substrate.

To evaluate the shifts in our spectra, we used an algorithm similar to the method introduced by Dahlin et al.[41] Instead of just tracking the minimum of the resonance, which is severely susceptible to noise and fluctuations, we calculate the centroid of the area enclosed by the resonance curve and a horizontal line given by a threshold value. This value was set once per measurement series and was defined by $T_{\mathrm{threshold}} = T_{\mathrm{min}} + \Delta T$, with $\Delta T \approx 0.1$ in absolute transmittance units, and T_{min} being the transmittance minimum of the reference spectrum.

AUTHOR INFORMATION

Corresponding Author

*E-mail: h.giessen@pi4.uni-stuttgart.de.

Notes

The authors declare no competing financial interest.

ACKNOWLEDGMENTS

The authors thank M. Hentschel, D. Dregely, and X. Yin for fabrication of the plasmonic structures, M. Ubl for technical assistance, F. Neubrech for discussions and comments, and Ph. Jordan for his valuable support. We acknowledge financial support by Baden-Württemberg Stiftung and the Ministerium für Wissenschaft, Forschung und Kunst Baden- Württemberg, as well as ERC (ComplexPlas), BMBF, DFG, and Carl-Zeiss-Stiftung. C.Z. and P.V.B. additionally acknowledge financial support from the Defense Threat Reduction Agency under award number HDTRA 1-12-1-0035.

REFERENCES

(1) Larsson, E. M.; Syrenova, S.; Langhammer, C. Nanoplasmonic Sensing for Nanomaterials Science. *Nanophotonics* **2012**, *1*, 249−266.

(2) Anker, J. N.; Hall, W. P.; Lyandres, O.; Shah, N. C.; Zhao, J.; Van Duyne, R. P. Biosensing with Plasmonic Nanosensors. *Nat. Mater.* **2008**, *7*, 442−453.

(3) Mayer, K. M.; Hafner, J. H. Localized Surface Plasmon Resonance Sensors. *Chem. Rev.* **2011**, *111*, 3828−3857.

(4) Hao, F.; Sonnefraud, Y.; Van Dorpe, P.; Maier, S. A.; Halas, N. J.; Nordlander, P. Symmetry Breaking in Plasmonic Nanocavities: Subradiant LSPR Sensing and a Tunable Fano Resonance. *Nano Lett.* **2008**, *8*, 3983−3988.

(5) Gallinet, B.; Martin, O. J. F. Refractive Index Sensing with Subradiant Modes: A Framework To Reduce Losses in Plasmonic Nanostructures. *ACS Nano* **2013**, *7*, 6978−6987.

(6) Jakab, A.; Rosman, C.; Khalavka, Y.; Becker, J.; Trügler, A.; Hohenester, U.; Sönnichsen, C. Highly Sensitive Plasmonic Silver Nanorods. *ACS Nano* **2011**, *5*, 6880−6885.

(7) Lazarides, A. A.; Kelly, K. L.; Jensen, T. R.; Schatz, G. C. Optical Properties of Metal Nanoparticles and Nanoparticle Aggregates Important in Biosensors. *J. Mol. Struct.: THEOCHEM* **2000**, *529*, 59−63.

(8) Mcmahon, J. M.; Henzie, J.; Odom, T. W.; Schatz, G. C.; Gray, S. K. Tailoring the Sensing Capabilities of Nanohole Arrays in Gold Films with Rayleigh Anomaly-Surface Plasmon Polaritons. *Opt. Express* **2007**, *15*, 18119−18129.

(9) Haes, A. J.; Zou, S.; Schatz, G. C.; Van Duyne, R. P. A Nanoscale Optical Biosensor: The Long Range Distance Dependence of the Localized Surface Plasmon Resonance of Noble Metal Nanoparticles. *J. Phys. Chem. B* **2004**, *108*, 109−116.

(10) König, M.; Rahmani, M.; Zhang, L.; Lei, D. Y.; Roschuk, T. R.; Giannini, V.; Qiu, C.-W.; Hong, M.; Schlücker, S.; Maier, S. A. Unveiling the Correlation between Nanometer-Thick Molecular

DOI: 10.1021/acsphotonics.5b00004
ACS Photonics 2015, 2, 475−480

Monolayer Sensitivity and Near-Field Enhahncement and Localization in Coupled Plasmonic Oligomers. *ACS Nano* **2014**, *8*, 9188−9198.
(11) Zhan, Y.; Lei, D. Y.; Li, X.; Maier, S. A. Plasmonic Fano Resonances in Nanohole Quadrumers for Ultra-Sensitive Refractive Index Sensing. *Nanoscale* **2014**, *6*, 4705−4715.
(12) Haynes, C. L.; Van Duyne, R. P. Nanosphere Lithography: A Versatile Nanofabrication Tool for Studies of Size-Dependent Nanoparticle Optics. *J. Phys. Chem. B* **2001**, *105*, 5599−5611.
(13) Guo, L. Nanoimprint Lithography: Methods and Material Requirements. *Adv. Mater.* **2007**, *19*, 495−513.
(14) Aksu, S.; Yanik, A. A.; Adato, R.; Artar, A.; Huang, M.; Altug, H. High-Throughput Nanofabrication of Infrared Plasmonic Nano-antenna Arrays for Vibrational Nanospectroscopy. *Nano Lett.* **2010**, *10*, 2511−2518.
(15) Yanik, A. A.; Huang, M.; Artar, A.; Chang, T.-Y.; Altug, H. Integrated Nanoplasmonic-Nanofluidic Biosensors with Targeted Delivery of Analytes. *Appl. Phys. Lett.* **2010**, *96*, 021101.
(16) Yanik, A. A.; Huang, M.; Kamohara, O.; Artar, A.; Geisbert, T. W.; Connor, J. H.; Altug, H. An Optofluidic Nanoplasmonic Biosensor for Direct Detection of Live Viruses from Biological Media. *Nano Lett.* **2010**, *10*, 4962−4969.
(17) Raschke, G.; Kowarik, S.; Franzl, T.; Sönnichsen, C.; Klar, T. A.; Feldmann, J.; Nichtl, A.; Kürzinger, K. Biomolecular Recognition Based on Single Gold Nanoparticle Light Scattering. *Nano Lett.* **2003**, *3*, 935−938.
(18) Buso, D.; Busato, G.; Guglielmi, M.; Martucci, A.; Bello, V.; Mattei, G.; Mazzoldi, P.; Post, M. L. Selective Optical Detection of H_2 and CO with SiO_2 Sol-Gel Films Containing NiO and Au Nanoparticles. *Nanotechnology* **2007**, *18*, 475505.
(19) Szunerits, S.; Boukherroub, R. Sensing Using Localised Surface Plasmon Resonance Sensors. *Chem. Commun.* **2012**, *48*, 8999−9010.
(20) Ando, M.; Kobayashi, T.; Iijima, S.; Haruta, M. Optical CO Sensitivity of Au-CuO Composite Film by Use of the Plasmon Absorption Change. *Sens. Actuators B* **2003**, *96*, 589−595.
(21) Kreno, L. E.; Hupp, J. T.; Van Duyne, R. P. Metal−Organic Framework Thin Film for Enhanced Localized Surface Plasmon Resonance Gas Sensing. *Anal. Chem.* **2010**, *82*, 8042−8046.
(22) Rosman, C.; Prasad, J.; Neiser, A.; Henkel, A.; Edgar, J.; Sönnichsen, C. Multiplexed Plasmon Sensor for Rapid Label-Free Analyte Detection. *Nano Lett.* **2013**, *13*, 3243−3247.
(23) Neubrech, F.; Pucci, A.; Cornelius, T.; Karim, S.; García-Etxarri, A.; Aizpurua, J. Resonant Plasmonic and Vibrational Coupling in a Tailored Nanoantenna for Infrared Detection. *Phys. Rev. Lett.* **2008**, *101*, 157403.
(24) Stuart, D. A.; Yuen, J. M.; Shah, N.; Lyandres, O.; Yonzon, C. R.; Glucksberg, M. R.; Walsh, J. T.; Van Duyne, R. P. In Vivo Glucose Measurement by Surface-Enhanced Raman Spectroscopy. *Anal. Chem.* **2006**, *78*, 7211−7215.
(25) Weissman, J. M.; Sunkara, H. B.; Tse, A. S.; Asher, S. A. Thermally Switchable Periodicities and Diffraction from Mesoscopically Ordered Materials. *Science* **1996**, *274*, 959−960.
(26) Tanaka, T.; Fillmore, D.; Sun, S.-T.; Nishio, I.; Swislow, G.; Shah, A. Phase Transitions in Ionic Gels. *Phys. Rev. Lett.* **1980**, *45*, 1636−1639.
(27) Kataoka, K.; Koyo, H.; Tsuruta, T. Novel pH-Sensitive Hydrogels of Segmented Poly(amine ureas) Having a Repetitive Array of Polar and Apolar Units in the Main Chain. *Macromolecules* **1995**, *28*, 3336−3341.
(28) Lee, K.; Asher, S. A. Photonic Crystal Chemical Sensors: pH and Ionic Strength. *J. Am. Chem. Soc.* **2000**, *122*, 9534−9537.
(29) Alexeev, V. L.; Sharma, A. C.; Goponenko, A. V.; Das, S.; Lednev, I. K.; Wilcox, C. S.; Finegold, D. N.; Asher, S. A. High Ionic Strength Glucose-Sensing Photonic Crystal. *Anal. Chem.* **2003**, *75*, 2316−2323.
(30) Asher, S. A.; Peteu, S. F.; Reese, C. E.; Lin, X.; Finegold, D. Polymerized Crystalline Colloidal Array Chemical-Sensing Materials for Detection of Lead in Body Fluids. *Anal. Bioanal. Chem.* **2002**, *373*, 632−638.
(31) Miyata, T.; Asami, N.; Uragami, T. A Reversibly Antigen-Responsive Hydrogel. *Nature* **1999**, *399*, 766−769.
(32) Watanabe, M.; Akahoshi, T.; Tabata, Y.; Nakayama, D. Molecular Specific Swelling Change of Hydrogels in Accordance with the Concentration of Guest Molecules. *J. Am. Chem. Soc.* **1998**, *120*, 5577−5578.
(33) Lee, Y.-J.; Pruzinsky, S. A.; Braun, P. V. Glucose-Sensitive Inverse Opal Hydrogels: Analysis of Optical Diffraction Response. *Langmuir* **2004**, *20*, 3096−3106.
(34) Liu, N.; Weiss, T.; Mesch, M.; Langguth, L.; Eigenthaler, U.; Hirscher, M.; Sönnichsen, C.; Giessen, H. Planar Metamaterial Analogue of Electromagnetically Induced Transparency for Plasmonic Sensing. *Nano Lett.* **2010**, *10*, 1103−1107.
(35) Zhang, C.; Losego, M. D.; Braun, P. V. Hydrogel-Based Glucose Sensors: Effects of Phenylboronic Acid Chemical Structure on Response. *Chem. Mater.* **2013**, *25*, 3239−3250.
(36) Gabai, R.; Sallacan, N.; Chegel, V.; Bourenko, T.; Katz, E.; Willner, I. Characterization of the Swelling of Acrylamidophenylboronic Acid - Acrylamide Hydrogels upon Interaction with Glucose by Faradaic Impedance Spectroscopy, Chronopotentiometry, Quartz-Crystal Microbalance (QCM), and Surface Plasmon Resonance (SPR) Experiments. *J. Phys. Chem. B* **2001**, *105*, 8196−8202.
(37) Hsieh, H. V.; Pfeiffer, Z. A.; Amiss, T. J.; Sherman, D. B.; Pitner, J. B. Direct Detection of Glucose by Surface Plasmon Resonance with Bacterial Glucose/Galactose-Binding Protein. *Biosens. Bioelectron.* **2004**, *19*, 653−660.
(38) Ersöz, A.; Denizli, A.; Özcan, A.; Say, R. Molecularly Imprinted Ligand-Exchange Recognition Assay of Glucose by Quartz Crystal Microbalance. *Biosens. Bioelectron.* **2005**, *20*, 2197−2202.
(39) Alexeev, V. L.; Das, S.; Finegold, D. N.; Asher, S. A. Photonic Crystal Glucose-Sensing Material for Noninvasive Monitoring of Glucose in Tear Fluid. *Clin. Chem.* **2004**, *50*, 2353−2360.
(40) Li, S.; Davis, E. N.; Anderson, J.; Lin, Q.; Wang, Q. Development of Boronic Acid Grafted Random Copolymer Sensing Fluid for Continuous Glucose Monitoring. *Biomacromolecules* **2009**, *10*, 113−118.
(41) Dahlin, A. B.; Tegenfeldt, J. O.; Höök, F. Improving the Instrumental Resolution of Sensors Based on Localized Surface Plasmon Resonance. *Anal. Chem.* **2006**, *78*, 4416−4423.

DOI: 10.1021/acsphotonics.5b00004
ACS Photonics 2015, 2, 475−480